JOURNAL OF Applied Polymer SCIENCE

Synthesis and Reactive Features of a Terpolymer: Poly(*N*-vinyl-2-pyrrolidone-*co*-vinyl acetate-*co*-glycidyl methacrylate)

David K. Hood,[1] David E. Kranbuehl,[2,3] A. Jaeton Glover,[2,3] Laurence Senak,[1] Chao Zhu,[1] Seher Ozkan,[1] Osama M. Musa[1]

[1]Ashland Specialty Ingredients (ASI), Wayne, New Jersey 07470

[2]Department of Applied Science, The College of William and Mary, Williamsburg, Virginia 23187

[3]Department of Chemistry, The College of William and Mary, Williamsburg, Virginia 23187

Correspondence to: D. K. Hood (E-mail: dhood@ashland.com)

ABSTRACT: A polyvinyl pyrrolidone terpolymer system is described that can be chemically cross-linked at moderate, 70–100°C, temperatures. The system has significant potential for development of durable long-lasting pyrrolidone coatings in a wide range of applications, particularly in water filtration membrane construction where leaching is an unresolved, serious problem. The synthesis of the terpolymer, poly(*N*-vinyl-2-pyrrolidone-*co*-vinyl acetate-*co*-glycidyl methacrylate), by free radical polymerization is described. The reactive features of this terpolymer are presented in the context of acidic anhydride curing. In a polar aprotic solvent, the terpolymer is reacted with poly(methyl vinyl ether-*co*-maleic acid) and cured thermally. Key aspects of the terpolymer synthesis and the acid anhydride cross-linking reaction using DSC, rheology, FTIR, and a small molecule model system to study the cross-linking chemistry are presented. © 2012 Wiley Periodicals, Inc. J. Appl. Polym. Sci. 000: 000–000, 2012

KEYWORDS: poly(vinyl pyrrolidone-*co*-vinyl acetate-*co*-glycidyl methacrylate); reactive polymer; membranes; hydrophilic polymers; cross-linking; properties and characterization

Received 20 March 2012; accepted 29 June 2012; published online
DOI: 10.1002/app.38287

INTRODUCTION

Commercial production of polyvinyl pyrrolidone (PVP), a polyvinyl lactam, has existed for more than 50 years. Since the early days of production, these materials have experienced strong commercial growth and acceptance in a myriad of applications. Among the most significant industrial applications are dispersants, adhesives, functional hydrophilic coatings, personal care applications, ink/dye receptive surfaces, membrane additives, and pharmaceutical excipients.[1] A key property of PVP is its hygroscopic, water-soluble nature. This property can vary somewhat as a function of molecular weight, but even very high molecular weight PVP is quite water-soluble. Another important attribute of PVP is complexation. PVP is capable of complexing many different materials. Polyacids, phenols, aromatics, iodine, and dyes are all well-known. Many of these complexing interactions are due to the strong hydrogen bonding and linear aliphatic backbone of the polymer[2,3] (Figure 1).

However, despite the unique structure and functionality of PVP, the water-solubility continues to be a significant limitation in some applications.

This article focuses on a system that resembles the important commercial membrane construction and application. The technical demands of water treatment via membrane filtration are increasing. Recently, Voith reported that waste water treatment is an important industrial challenge because of regulatory pressures to treat these waters prior to discharge into the environment.[4] In water filtration membrane constructions, PVP is known as an effective agent for porosity and permeability improvement via enhancements to the hydrophilic properties of well-known membrane substrates such as polysulfones and polyvinylidene fluorides.[5–7] Although useful, over time the PVP leaches out of the membrane. As a result, the membrane becomes more hydrophobic, with the result that it becomes more prone to fouling and less permeable.[6] New techniques for chemically incorporating PVP into membrane substrates will eliminate leaching, enhance the performance of these polymer membranes and provide new approaches to this demanding application.

Various strategies for enhancing the water resistance of lactamic functionality have been previously employed. First, copolymerization with hydrophobic monomers, such as vinyl acetate (VA)

Applied Polymer SCIENCE

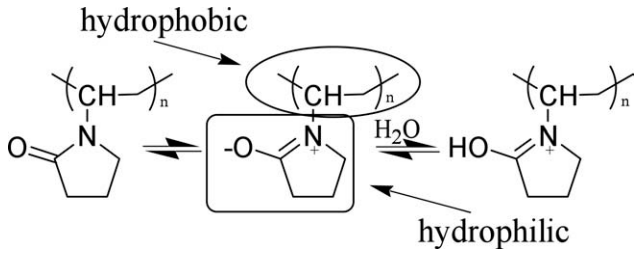

Figure 1. Various functional features of poly(*N*-vinyl-2-pyrrolidone) (PVP), a polyvinyl lactam.[2,3]

and lauryl methacrylate, is a common approach. For example, a poly(vinyl pyrrolidone-*co*-vinyl acetate) (PVP/VA) polymer ratio of 70/30 is water soluble in contrast to a 30/70 ratio, which is water insoluble but continues to exhibit moisture sensitivity. The PVP/VA copolymer ratio has been more broadly expanded to provide further possibilities in hydrophilic/hydrophobic balance. However, these copolymers remain soluble in solvents such as alcohol, and can be susceptible to leaching or migration. A second strategy previously employed is introduction of a cross-linker to a receptive lactamic copolymer. Although effective, there are challenges to this approach. Suitable cross-linkers, coating formulation stabilization (where the cross-linker is present in the premanufactured solution), and safe handling of such materials in a production environment are all major challenges.[8,9] A third strategy has been to employ photo-irradiation processes to hydrophilic monomers, such as vinyl pyrrolidone, to form cross-linked, hydrophilic functional membrane surfaces, especially membranes comprised of polysulfones.[10] Polysulfones are photo-sensitive and capable of generating free radicals upon exposure to UV irradiation.[11] This type of UV process enables membrane surface functionalization by "photo-grafting," via polymerization initiated from the membrane polymer or grafting of monomers employing traditional photo-initiators. Although effective in certain cases, there are several important challenges with such approaches. For example, care must be taken to manage the important physical and morphological changes resulting from exposing the membrane to UV irradiation, especially for critical parameters such as pore size.[10] In addition, from a safety perspective, implementation of "dip methods" or classic coating methods in large processes can result in subjecting personnel to exposure to monomers, which is often not desirable. Here, we discuss the potential for inclusion of a thermally cross-linkable, reactive polymer, incorporating the functionality to PVP, but that also addresses many of these important concerns.

A few examples of reactive PVP copolymers can be found in the literature. Reddy and Soundararajan describe the synthesis and characterization of poly(*N*-vinyl-2-pyrrolidone-*co*-glycidyl methacrylate) (PVP/GMA) in chloroform.[12] Sukhishvili and Qiu describe the synthesis and characterization of poly(*N*-vinyl caprolactam-*co*-glycidyl methacrylate) (PVCL/GMA) in dioxane.[13] They further grafted the PVCL/GMA polymer with amino-terminated polyethylene oxide (PEO). PVP/GMA, made via a precipitation route in ethyl acetate or toluene, has been reported by Mathauer et al.[14] Nagaoka and Akashi describe a terpolymer of poly(*N*-vinyl-2-pyrrolidone-*co*-vinyl acetate-*co*-glycidyl acrylate) [P(VP-VA-GA)] prepared in isopropanol via a tube polymerization process and purified by precipitation, resulting in yields ranging from 70 to 90%.[15] Many of these possibilities are commercially impractical, or at least inconvenient, polymerization routes.

The functionality of reactive PVP has not been rigorously studied and reported. The focus of this article is to present not only the solution synthesis of a reactive terpolymer poly(*N*-vinyl-2-pyrrolidone-*co*-vinyl acetate-*co*-glycidyl methacrylate) [P(VP-VA-GMA)] but also to study the key reactive functional aspects of this terpolymer with polymeric acids.[16,17] A proposed general reaction scheme for the cross-linking of P(VP-VA-GMA) with poly(methyl vinyl ether-*co*-maleic acid) [P(MVE-MA)] is presented in Figure 2.

We also report on important practical problems such as reactivity of the P(VP-VA-GMA) polymer at lower temperatures, specifically 60–80°C, coupled to understanding the important polymer reaction mechanisms toward polymeric acids in this temperature range.

EXPERIMENTAL

Materials

N-Vinyl-2-pyrrolidone (VP; 99 min. purity), *N*-methyl-2-pyrrolidone (NMP; 99+% purity), and poly(methyl vinyl ether-*co*-maleic acid) [P(MVE-MA); Gantrez S-97 powder] were obtained from Ashland Specialty Ingredients (ASI) (Wayne, New Jersey). Glycidyl methacrylate (GMA; 97% purity), vinyl acetate (VA; 99+% purity), and acetone (ACS Reagent Grade) were obtained from Aldrich (Milwaukee, Wisconsin). *tert*-Butyl

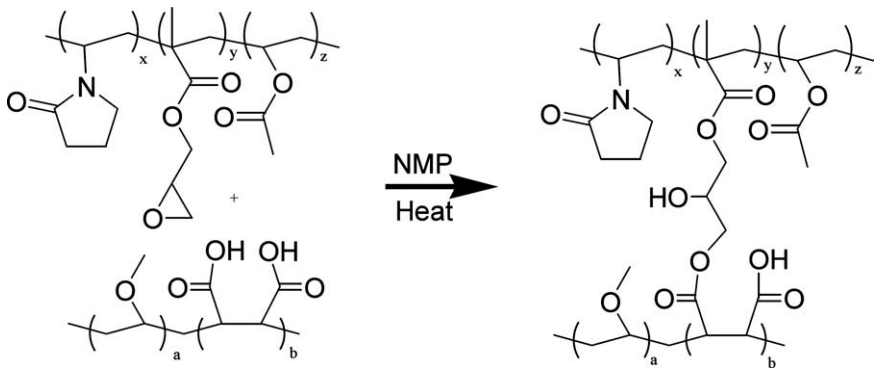

Figure 2. Proposed general reaction scheme for P(VP-VA-GMA) and P(MVE-MA) in NMP.

peroxypivalate, 75% solution in mineral spirits (Trigonox 25-C75) was obtained from Akzo Nobel (Chicago, Illinois). All materials were used as-received.

Synthesis of Poly[(N-vinyl-2-pyrrolidone)-co-vinyl acetate-co-glycidyl methacrylate] P(VP-VA-GMA)[18]

P(VP-VA-GMA) was prepared via a solution-free radical polymerization process. A typical polymer of 110 g of terpolymer is described. A feed of VP (70 g, 0.630 mol) and GMA (30 g, 0.211 mol) is prepared for pumping. A second feed of VA (10 g, 0.116 mol) is prepared in a second pump. In another vessel, a mixture of Trigonox 25-C75 (1 g, 0.0043 mol) and 5 g of acetone is prepared as the initiator solution. Two hundred thirteen grams of acetone is charged to a three-necked, round bottom flask equipped with a magnetic stirrer, nitrogen inlet, and a condenser. The flask is purged with nitrogen for ~ 20 min followed by heating to reflux, ~ 55°C, while maintaining the nitrogen sparge. When the flask achieves the reflux temperature, the VP/GMA (~ 0.8 mL/min) and VA (~ 0.1 mL/min) feeds commence. After 10 min of the initial monomer feed, a 1 g sample of the initiator solution is charged into the flask. Although the monomers are fed into the reactor, after 30, 60, and 90 min, another 1 g of initiator solution is charged into the flask. At the completion of the monomer feeds, the flask receives another 1 g charge of initiator solution. The reaction vessel is allowed to heat at reflux an additional 3 h. The flask is then charged Trigonox 25-C75 (0.5 g, 0.00215 mol) held for 2 h. A final charge of Trigonox 25-C75 (0.5 g, 0.00215 mol) is then added and the flask held for 5 h and allowed to cool. Note that during this process, additional acetone was added to replace any that had volatilized. The total residual monomers, as determined by gas chromatography, is ~ 0.5% (wt %). To the terpolymer in acetone, the desired solvent medium is added, followed by vacuum removal of acetone. This step was employed to enable the presentation of the terpolymer in the desired amount of NMP for further study.

Methods

Molecular Weight Distribution Determination. Molecular weight distribution measurements from gel permeation chromatography (GPC) of the precured terpolymers were made using a Waters GPC (Milford, Massachusetts) system equipped with an isocratic solvent delivery system and a refractive index detector. The samples were separated by size with a single linear Shodex (New York, New York) OH-Pak SB806-MHQ GPC column. The chromatography employed a mobile phase that was 50/50 water/methanol (v/v) made 0.4 *M* with $LiNO_3$, 0.1 *M* with Tris, and adjusted to pH-9 with nitric acid. The flow rate was 0.5 mL/min and the sample concentration was 0.15% (w/v). Molecular weight distributions are reported relative to PEO standards from Polymer Laboratories (Amherst, Massachusetts).

Differential Scanning Calorimetry. DSC data were acquired with a TA Instruments (New Castle, Delaware) DSC 2920 calorimeter under nitrogen, in a heating cycle from 30 to 250°C using a scanning rate of 10°C or under indicated isothermal conditions.

FTIR Spectroscopic Characterization. Infrared spectroscopy was accomplished using a Thermo (Waltham, Massachusetts) 6700 FTIR spectrophotometer, equipped with a DTGS detector and a thermostatically controlled Harrick cell. Sample solutions for curing were placed NEAT between two 2 × 25 mm NaCl windows without Teflon spacers. The temperature was gradually ramped to 180°C and the resulting spectra were obtained. Spectra were obtained at 4 cm^{-1} resolution, under dry air purge with the coaddition of 32 interferograms. These were apodized with a triangular function and Fourier-transformed with one level of zero filling to yield data encoded every 2 cm^{-1}. Quantification of band intensities was accomplished by transferring data from the instrument to a computer using GRAMS software. The baseline was flattened between nominally 780 and 715 cm^{-1}. Peak heights were then compared between the GMA epoxide band at 765 cm^{-1} and the band resulting from NMP at 746 cm^{-1}.

Rheological Characterization. Rheological characterization was performed with an AR-G2 rheometer (TA Instruments) with a couette flow configuration to accomplish multiwave dynamic oscillatory flow experiments. Strain amplitude was 0.5% and the frequencies were 0.5, 1, and 5 Hz for one case (60°C study) and 0.5, 1, and 10 Hz for the rest of the cases. Initial work was performed as to ensure that responses were in the linear viscoelastic region during the curing process (strain sweep tests).

RESULTS AND DISCUSSION

Molecular weight distributions as obtained from GPC chromatography provide weight average molecular weights (M_w) for batches of the P(VP-VA-GMA) terpolymer used in the gel curing that range from 30,000 to 50,000 amu relative to poly(ethylene oxide) standards. Polydispersities (M_w/M_n) ranged from 4.0 to 6.0 for these polymers. Typical P(MVE-MA) weight average molecular weights as obtained from GPC using PEO calibration are nominally 1 million with polydispersities in the range of 7. These are the polymers used to form the reactive matrix in making the cross-linked gel products.

A reactive matrix of P(VP-VA-GMA) (36.7%), P(MVE-MA) (8.3%), and NMP (55%) was prepared at room temperature for further study. This system was designed to enable the exploration of acid anhydride curing of an epoxide polymer in the presence of tertiary amine (Lewis Base) catalyst.

DSC Characterization

A variety of DSC experiments were designed to elucidate the complex thermodynamic events observed for this reactive matrix. To separate these events, the components were first evaluated in binary fashion. P(MVE-MA) and NMP were mixed, at 45%, and tested as displayed in Figure 3(A, B).

It was observed that a "freshly" prepared solution exhibited an exothermic event between 40°C and 60°C. This event was not observed when the sample was aged for ~ 12 h. A second exothermic event was also observed, in both samples, in the higher temperature range of 120–170°C, with the "fresh" sample exhibiting a notably higher result. The "low" temperature event is attributed to the neutralization effects of the NMP to the maleic acid component of P(MVE-MA).

A similar set of experiments were also performed on the P(VP-VA-GMA) and NMP system. In this case, an exotherm was observed in the range of 80–140°C, indicative of epoxide polymerization. A much stronger exothermic event is observed to

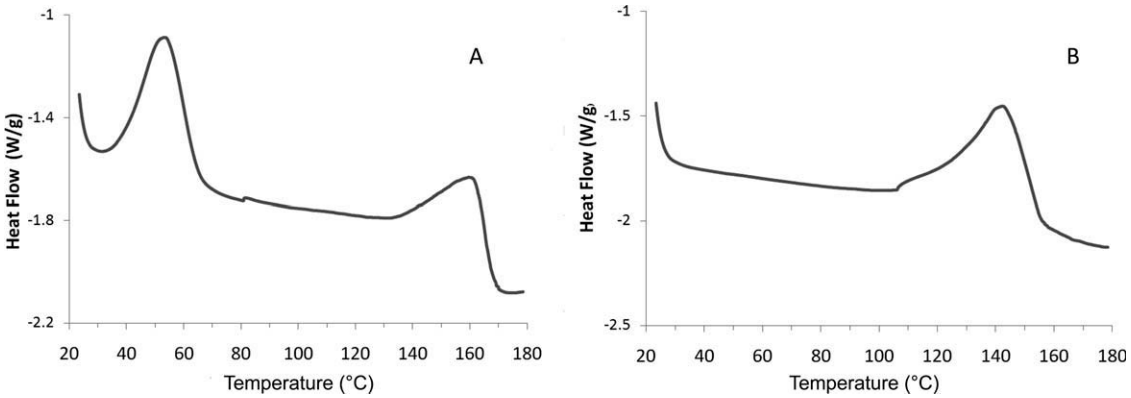

Figure 3. DSC thermogram for (Panel A) P(MVE-MA) at 45% solids in a freshly prepared solution, and for (Panel B) the same solution aged 12 h.

begin at >150°C, but was not studied further as this was outside of range of interest.

In the completed reactive matrix, where P(VP-VA-GMA) + P(MVE-MA) + NMP are in place [Figure 4(A, B)], a freshly prepared sample exhibits the lower temperature exotherm in the range of 40–60°C, which disappears upon aging after ~ 12 h.

Again, a second exothermic event was also observed, in both samples, in the higher temperature range of 120–170°C, with the "fresh" sample exhibiting a notably higher result.*

The heat capacity of the reactive matrix was also evaluated at 80, 100, 120, and 140°C. This was accomplished using modulated DSC at each temperature. The heat capacity is obtained as the result of measurement of modulation at regular intervals during the curing process around a constant temperature. In this case, the temperature modulation was 0.5°C at 45 s intervals. No changes in the heat capacity were observed below the 120°C experiment. At 120°C, the heat capacity was observed to change sharply at ~ 140 min. At 140°C, the heat capacity changes sharply at ~ 25 min. Key to these results is that the DSC was not capable of observing any "gel" events in the more modest temperatures of the desired work.

Rheological Characterization

In chemically cross-linked systems, the gel point marking the transition of the material from liquid to solid state is defined as the instant at which the weight average molecular weight diverges to infinity or at which the largest molecular cluster extends across the sample.[19] Before the gel point, molecules are cross-linked into small size clusters that are weak solids. These clusters, according to Cates,[20] can be defined as polymeric fractals with defects such as loose ends, loops, and unreacted cross-link sites. Percolation theory can be used to study this system.[21,22] The clusters get larger with increasing reaction time, until they form an infinite size cluster with a network that extends across the entire sample when it reaches the gel point. This transition from liquid to solid state is a gradual and continuous process that manifests itself in the viscoelastic behavior of the material. Gelation and vitrification, therefore, can be detected through the changes in the dynamic rheological properties of a material during isothermal curing. In this study, the curing behavior of the P(VP-VA-GMA)/P(MVE-MA)/NMP mixture is characterized by rheological measurements over a series of temperatures.

Rheological evaluation (multiwave oscillatory tests in the linear viscoelastic region) was obtained at three different temperatures at 60, 70, and 80°C. Strain amplitude was 0.5% and the frequencies utilized were 0.5, 1, and 10 Hz. Premixed samples were loaded into the rheometer at ambient temperature. Samples were then brought to one of the above experimental temperatures at a 10°C/min ramp rate. The change in storage modulus (G', Pa), loss modulus (G'', Pa), magnitude of complex viscosity (η^*, Pa s), and tan δ values were measured during heating and curing process. Solvent evaporation for all rheological experiments was found to be negligible based on weighing the sample before and after the test.

Prevalent in the literature is the establishment of the gel point at the point where the loss tangent (tan δ) becomes independent of the measurement frequency with tan δ being less than 1.[19,23,24] An example of work that utilizes the above relationship is that of Lange et al.[23] Typically, chemically cross-linked gels exhibit $G' > G''$ with both G' and G'' invariant as a function of frequency. Since tan $\delta = G''/G'$ with $G'>G''$ after the point of gelation, tan δ would be <1. A couette flow geometry was chosen to measure these parameters throughout the linear viscoelastic region for the whole curing process. For this reason, a low value for strain amplitude (0.5%) was chosen.

For the curing of the P(VP-VA-GMA)/P(MVE-MA)/NMP mixture, the change in storage modulus (G'), loss modulus (G''), and tan δ at the different temperatures (60, 70, and 80°C) as a function of time is displayed in Figures 5–7, respectively.

The sample begins as a liquid under ambient conditions with $G'' > G'$, demonstrating a system where gel has not yet formed. As the sample is ramped to temperature, a significant drop in loss and storage modulus is initially observed due to thermal effects. Figure 8 displays an expanded view of this effect.

*Thermogravimetric analysis (TGA) results demonstrate that on-set to weight loss is observed at ~ 90°C, as observed by a 5% loss in mass, indicating that the corresponding thermodynamic observations are not related to any deviations in the sample mass.

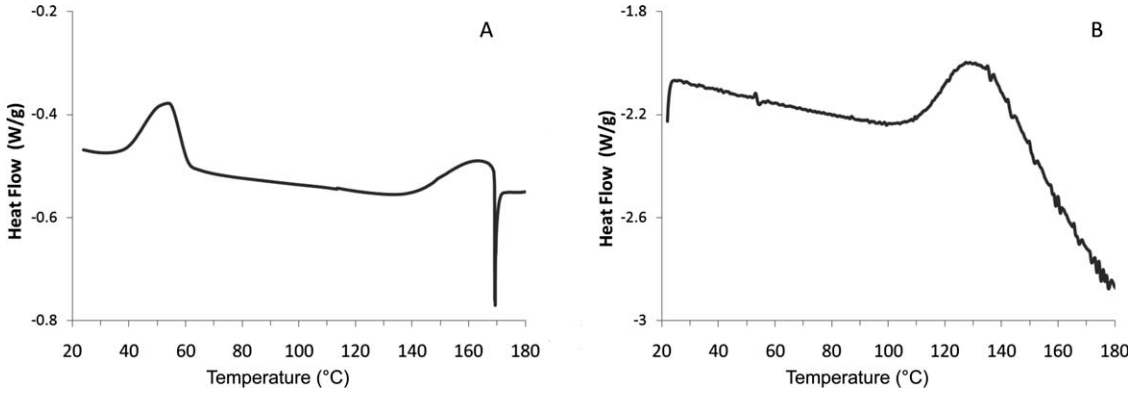

Figure 4. DSC thermogram for 45% solids [36.7% P(VP-VA-GMA)–8.3% P(MVE-MA)] in NMP heat flow (W/g) as a function of temperature for (Panel A) a freshly prepared solution, and (Panel B) aged for 12 h.

Subsequently it was seen in all three of the temperature experiments that G', G'', and Eta (magnitude of complex viscosity) all begin increasing at above 58°C (nominally 300 s into the experiment). This observation coincides with the DSC observation that shows an exothermic event between 40°C and 60°C for "freshly" prepared 45% binary solution. These values display a relatively rapid increase, followed by a plateau, followed by another increase of lesser slope. There was no cross-over observed for the 60°C experiment for the 3 h experiment duration. Tan δ values were greater than 1 for all of the frequencies tested. In contrast, gelation (cross-over) was observed for the 70°C curing temperature 205 min after the 300 s start, and at 27 min after the start time for the 80°C curing experiment. A potential inhibition of the curing of systems such as this has been speculated to lie in its mobility/viscosity.[23] To investigate such a possibility, the same 70°C experiment described above was performed with a 34% total solid system, with the ratio of solid components equivalent to the 45% solids system (data not shown). This lower solids system displayed a gel formation time of 131 min, somewhat shorter than the 205 min for the 45% solids system. This data would then support mobility/viscosity of reactive species as a factor affecting the time of gel formation and most likely the cross-link density of the terpolymer system.

It should also be noted that at 3–4 h at room temperature, a viscosity increase is observed. The nature of this viscosity increase was uncertain, particularly in light of the gain coming under ambient conditions. For this reason, an experiment was conducted for the system at 25°C (same testing parameters as curing experiments) for 3 h as displayed in Figure 9.

Again, no cross-over is observed, which may be indicating that this increase in viscosity is not due to a covalent cross-linking reaction that would form an irreversible percolated network structure. An increase in viscosity is also observed for a simple homo-polymer system of 45 wt % P(MVE-MA)/NMP. For this reason, the same parameters measured above were also monitored for the 45% binary system in Figure 10.

After 250 s, tan δ values for all three frequencies were less than 1, but not overlapping as a function of the frequency dependency of the tan δ values. This is considered an indication of noncovalent interactions as confirmed with gel solubility studies that demonstrated the gelation process of the P(MVE-MA) system to be reversible. Similar to chemically cross-linked systems, colloidal systems can also undergo a sol-gel (liquid to solid) transition that would produce the cross-over of storage modulus values of the sample at the gel point.[24,25] Starting from a liquid

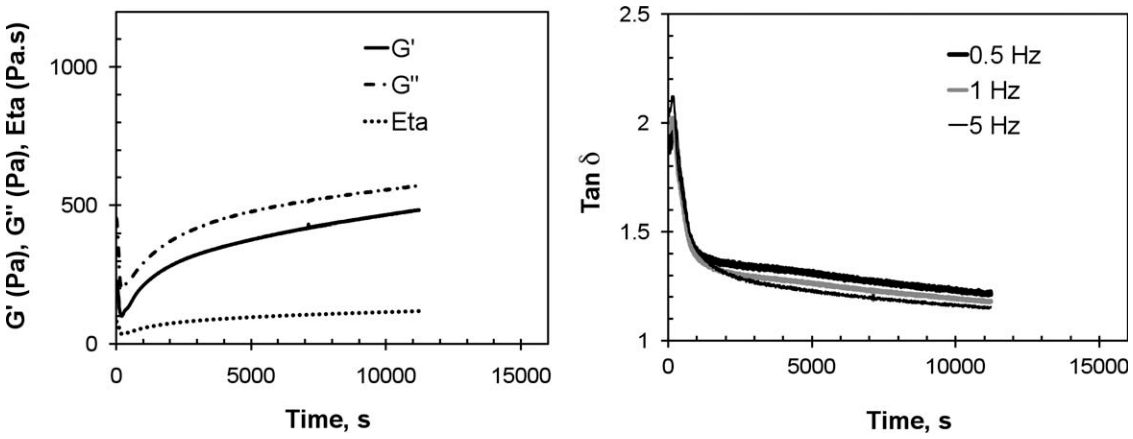

Figure 5. Rheological behavior measured at 60°C for 45% solids [36.7% P(VP-VA-GMA)–8.3% P(MVE-MA)] in NMP, G' (Pa), G''(Pa), magnitude of complex viscosity (Eta, Pa s) measured at 1 Hz frequency and 0.5% strain amplitude. Tan δ values are measured at 0.1, 1, and 5 Hz frequency.

Applied Polymer SCIENCE

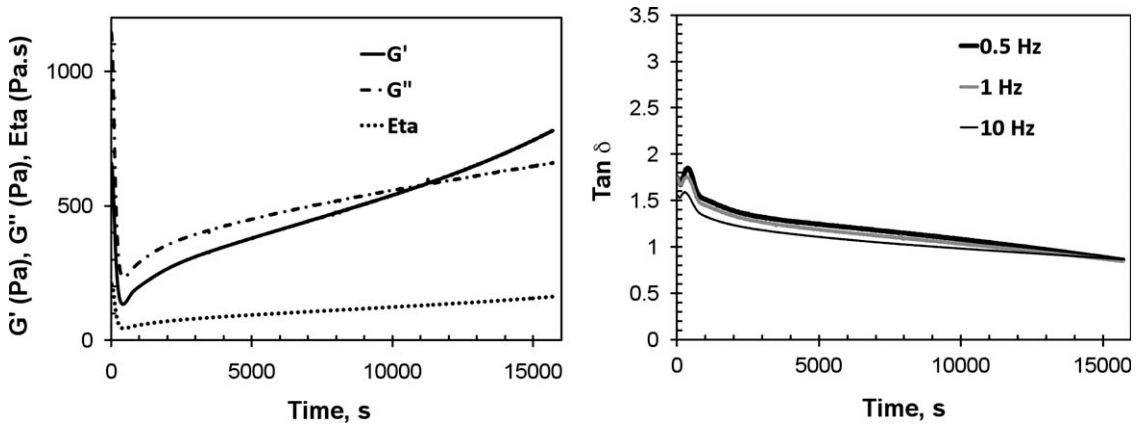

Figure 6. Rheological behavior measured at 70°C for 45% solids [36.7% P(VP-VA-GMA)–8.3% P(MVE-MA)] in NMP, G' (Pa), G'' (Pa), magnitude of complex viscosity (Eta, Pa s) measured at 1 Hz frequency and 0.5% strain amplitude. Tan δ values are measured at 0.1, 1, and 10 Hz frequency.

state, an increase in the volume fraction (ϕ) of the polymer molecules or clusters leads to the formation of ever growing aggregates due to weak particle–particle interactions. In this case, these weak particle–particle interactions may be due to either chemical structure of P(MVE-MA) and NMP or a kinetic effect such as increasing radius of hydration of P(MVE-MA) in time as it goes into solution in NMP.[26–28]

Once these aggregates span the system, the clusters that formed the network will be able to transmit stresses between the opposite sides of the system and there will be a sharp increase in the dynamic oscillatory response, specifically in the storage modulus (G') values of the material. This will cause a sol-gel transition.[25] The percolation theory can be used to model this system as long as the transient nature of these spanning aggregates is taken into account. Classical "snapshot" percolation theory, that considers the system with a spanned aggregate at any given time, may be acceptable for chemically cross-linked systems beyond gel point. In the case of colloidal gels, on the other hand, a spanning cluster may break up due to thermal agitation as another spanning cluster forms in the sample. The spanned cluster, then, has an infinitesimal lifetime. The minimum lifetime of the particle–particle bonds in the percolated cluster and the rate of applied deformation effect the transmission of the stress across the system. This makes the mechanical response of the material a function of frequency during oscillatory flow experiments.[25] Under these circumstances, tan δ values at gel point collected with different frequencies will not overlap even though they are less than one.

To confirm results of the viscoelastic experiments performed above, a series of simple solubility studies on the above-mentioned systems were performed under equivalent experimental temperatures and times. The results of these solubility studies are displayed in Table I.

In confirmation of rheological testing, systems cured at 70°C or greater formed insoluble swollen gels (indicating covalent bonding/cross-linking), while samples cured at 60°C or less formed gels that were ultimately soluble (indicating only physical bonds/interactions).

FTIR Experiments

Crucial to the understanding and monitoring of the thermally induced cross-linking process in the generation of a P(VP/VA/

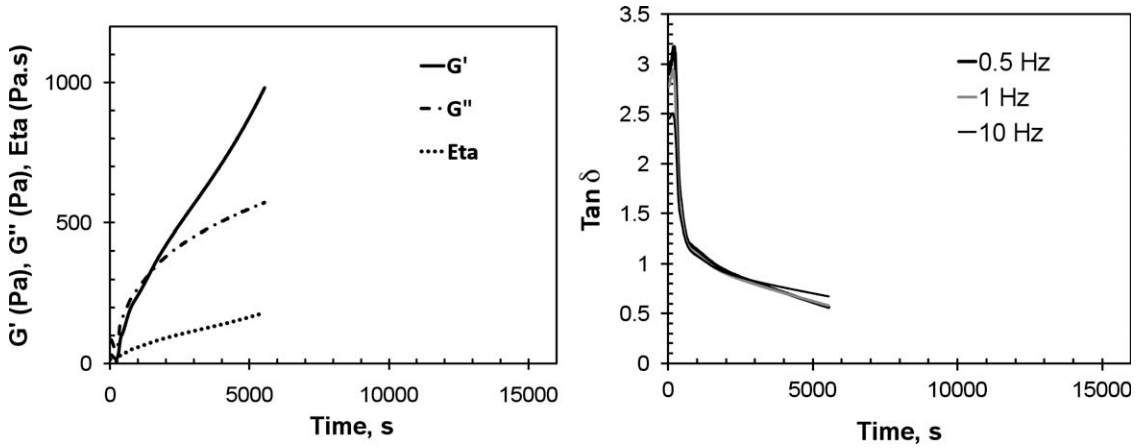

Figure 7. Rheological behavior measured at 80°C for 45% solids [36.7% P(VP-VA-GMA)–8.3% P(MVE-MA)] in NMP, G' (Pa), G'' (Pa), magnitude of complex viscosity (Eta, Pa s) measured at 1 Hz frequency and 0.5% strain amplitude. Tan δ values are measured at 0.1, 1, and 10 Hz frequency.

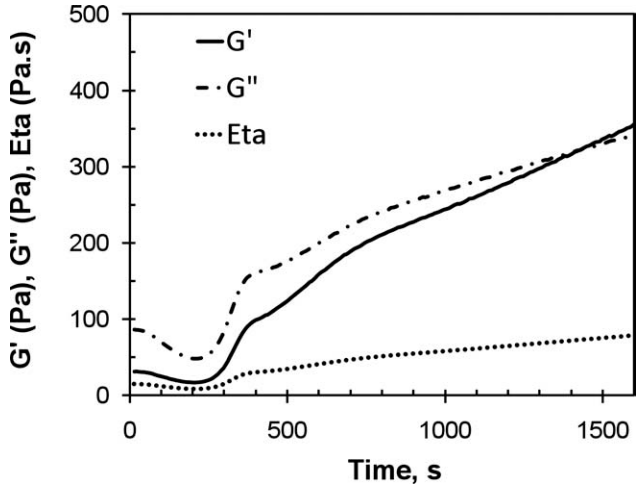

Figure 8. Expanded portion of the initial data presented in Figure 7; 80°C for 45% solids [36.7% P(VP-VA-GMA)–8.3% P(MVE-MA)] in NMP, G' (Pa), G'' (Pa), magnitude of complex viscosity (Eta, Pa s) measured at 1 Hz frequency and 0.5% strain amplitude.

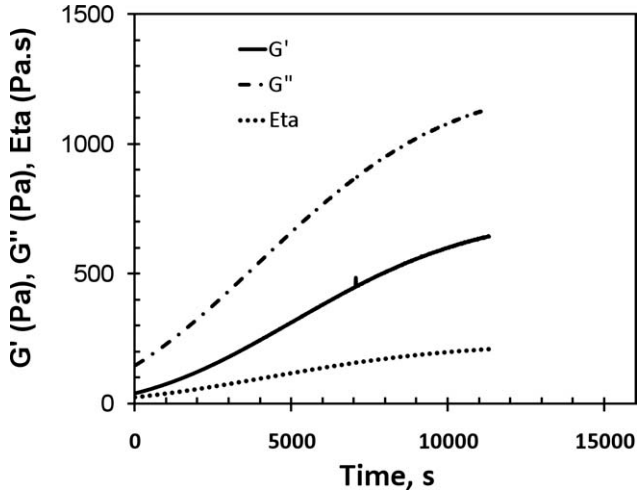

Figure 9. Rheological behavior measured at 25°C for 45% solids [36.7% P(VP-VA-GMA)–8.3% P(MVE-MA)] in NMP, G' (Pa), G'' (Pa), magnitude of complex viscosity (Eta, Pa s) measured at 1 Hz frequency and 0.5% strain amplitude.

GMA) and P(MVE-MA) gel network is the epoxide uptake from GMA in the curing event. FTIR is not only a valuable tool in both understanding and monitoring these reactions, it is also a logistically superior technique, not requiring aliquot sampling. Figure 11 displays the FTIR spectrum of a model compound mixture (GMA/MA) representing the above polymer mixture in NMP at 40°C and elevated temperatures.

This figure is an expanded range of the IR spectrum (700–800 cm^{-1}) to display the diminished epoxide band from GMA contribution to the spectrum at nominally 765 cm^{-1}. This diminishment of peak height at 765 cm^{-1} is indicative of epoxide consumption in the formation of covalent polymer cross-links. This observation has been previously noted and exploited in previous work.[29–31] Proposed general reaction schemes are displayed in Figure 12.

Quantification of the epoxide consumption can be accomplished cleanly in a set of model compound experiments employing maleic acid and GMA in NMP. NMP exhibits a band at 745 cm^{-1}, which can be used as an internal standard against which the consumption of the GMA epoxide can be quantified. Thus, the intensity ratio of ($I_{765\ cm^{-1}}/I_{745\ cm^{-1}}$) bands may be used to quantify epoxide consumption for these systems. The comparison of the intensity of these bands relative to each other is then displayed in Figure 12, and can be applied for both model compounds and the 45% solids polymer system in NMP. The FTIR experiment is then applied to both of the above-mentioned systems as a function of cure (reaction) temperature and time. Note that for the FTIR experiments, temperatures of 60, 80, and 100°C were used for quantification of the epoxide consumption. The results of these experiments are displayed in Figure 13.

From a kinetic standpoint, clear pictures of consumption of epoxide are presented for both the 60°C and 100°C experiments. For both the terpolymer system and the model compounds, the 60°C experiment indicates a relatively low

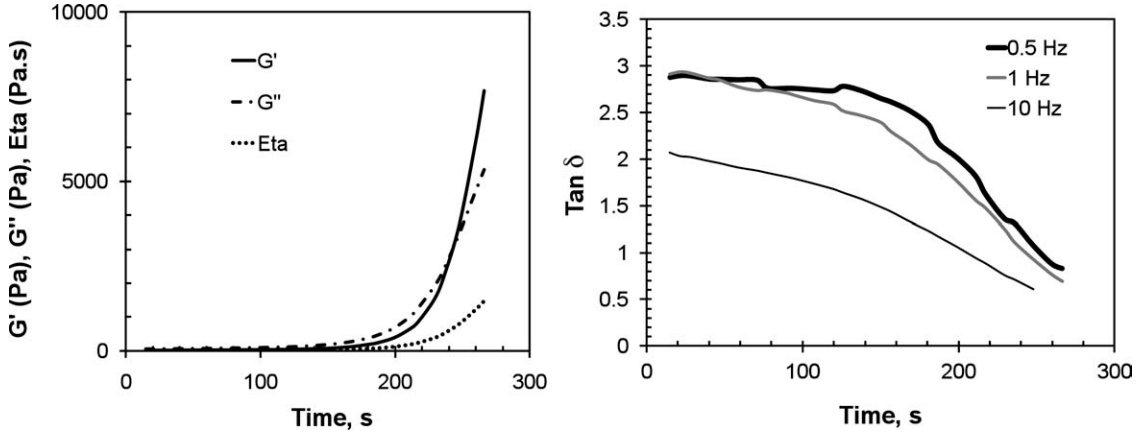

Figure 10. Rheological behavior measured at 60°C for 45% solids [45% P(MVE-MA)] in NMP, G' (Pa), G'' (Pa), magnitude of complex viscosity (Eta, Pa s) measured at 1 Hz frequency and 0.5% strain amplitude. Tan δ values are measured at 0.1, 1, and 10 Hz frequency.

Applied Polymer SCIENCE

Table I. Visual Observations in Support of Rheological Data

Material	Solvent	State
45% solids polymer system at 60°C for 3 h	NMP	Soluble
45% solids polymer system at 70°C for 4 h	NMP	Swollen polymer gel
45% solids polymer system at 80°C 1.5 h	NMP	Swollen polymer gel
34% solids polymer system at 70°C for 2.8 h	NMP	Swollen polymer gel
45% P(MVE-MA) in NMP at 25°C for 24 h	NMP	Soluble
45% P(MVE-MA) in NMP at 60°C for 4 min	NMP	Soluble
45 % P(MVE-MA) in NMP at 60°C for 4 min	Water	Soluble

consumption of epoxide. Here, it is less than 60% consumption for the model compounds and less than 50% consumption for the polymer system in an 8 h period. For the 100°C experiments, all of the epoxide is consumed relatively quickly (3–4 h for model compounds and 6 h for the polymer system). The intermediate temperature experiment of 80°C shows the greatest discrepancy for the consumption of epoxide between model compound and terpolymer system. For the model compounds, complete epoxide consumption is accomplished by about 6 h at slightly less of a rate than the 100°C experiment. In contrast, the terpolymer system only consumes about 60% of the epoxide by about 8 h.

The difference between model compounds and polymer at 80°C can be rationalized in terms of the relative viscosity/mobility of the two systems. There is little impedance for the reaction in the model system of the GMA epoxide and the maleic acid at 80°C temperature. In contrast, the terpolymer is under greater steric constraint for epoxide–poly(acid) reaction as the viscosity/mobility of the system increases as has been conveyed in the rheology discussion above. Although epoxide consumption within the terpolymer system may not be complete at 80°C, the amount of epoxide species needed to cross-link the system does not need to be near the 100% range of the model compound systems at 100°C. The FTIR study indicates that the amount of epoxide to acid cross-link, and therefore, cross-link density and

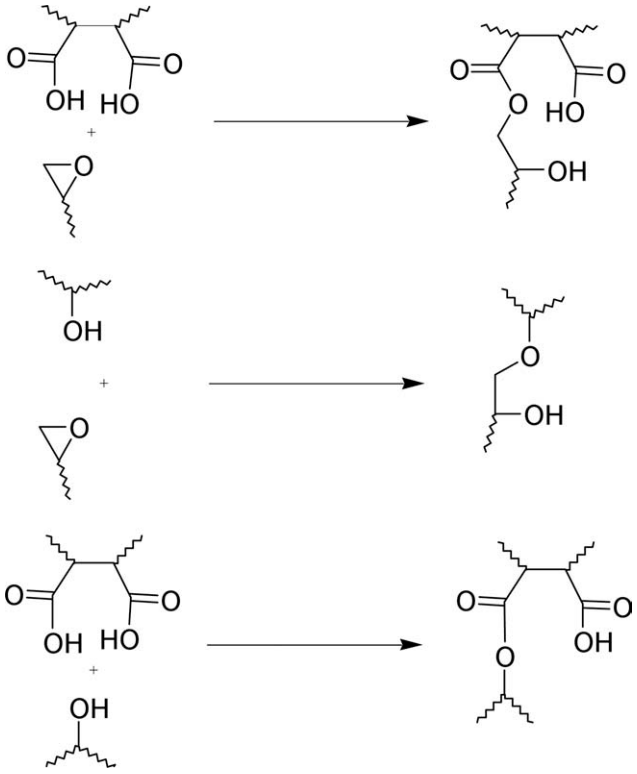

Figure 12. Proposed general reaction schemes for various cross-linking possibilities.[29]

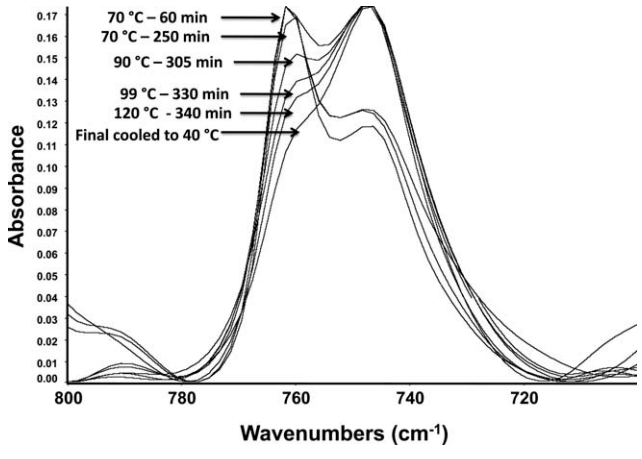

Figure 11. Expanded region of the FTIR spectrum of model compounds of (GMA/MA) in NMP. Epoxide band (765 cm^{-1}) diminishes as a function of temperature and can be compared to the intensity of the NMP band (745 cm^{-1}) taken as constant. ($I_{765\ cm^{-1}}/I_{745\ cm^{-1}}$) bands may be used to quantify epoxide consumption.

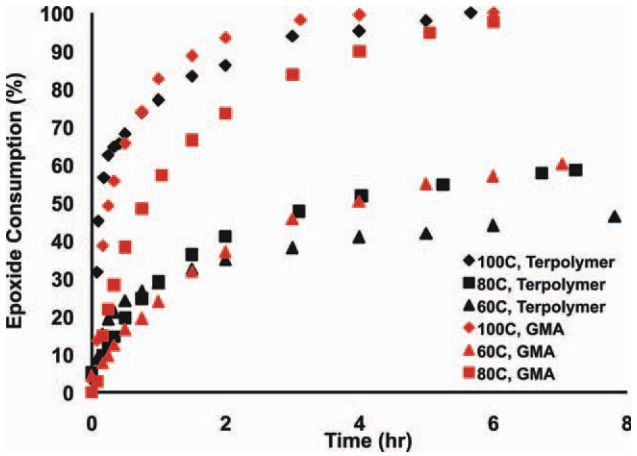

Figure 13. Epoxide consumption as a function of both time and temperature, for model compound (GMA/MA) and 45% solids [36.7% P(VP-VA-GMA)–8.3% P(MVE-MA)] in NMP. [Color figure can be viewed in the online issue, which is available at wileyonlinelibrary.com]

swell volume of the terpolymer system may be optimized by temperature and reaction time.

CONCLUSIONS

A terpolymer of vinyl pyrrolidone-*co*-vinyl acetate-*co*-glycidyl methacrylate [P(VP/VA/GMA)] has been successfully synthesized in acetone followed by removal and replacement with NMP. A system containing the P(VP/VA/GMA) terpolymer was reacted with p(methyl vinyl ether-*co*-maleic acid) copolymer (45% total polymer solids by weight) in the NMP solvent at a series of moderate, 70–100°C, temperatures to form cross-linked, irreversible gels.

To better describe this cross-linking process, analytical methods commonly employed to observe curing were evaluated for general suitability in such applications. DSC was determined to be incapable of observing any critical thermodynamic or gel formation events in the desired temperature range. The FTIR experiments were capable of observing epoxide consumption, but epoxide consumption alone cannot be directly related to gel formation, as evidenced by the 60°C and 80°C results. Rheology proved to be the most suitable technique for characterizing the formation of irreversible gels.

The implication of these results is that to develop a proper process model, FTIR techniques will need to be carefully developed in parallel with rheological techniques, most likely in well-defined temperature regimes. Subjects for future experiments include optimization of cross-link density and swell volume of gels resulting from the P(VP/VA/GMA)–P(MVE-MA)-NMP system as functions of temperature and solids concentration.

ACKNOWLEDGMENTS

The authors thank Donald Koelmel and Timothy Gillece for DSC and discussions, respectively. They also thank the management of Ashland Specialty Ingredients (ASI) for the opportunity to publish this work.

REFERENCES

1. Barabas, E. In Encyclopedia of Polymer Science and Engineering, 2nd ed.; Mark, H. F., Bikales, N. M., Overberger, C. C., Menges, G., Eds.; Wiley-Interscience: New York, **1999;** Vol. *17*, p 198.
2. Takagishi, T.; Kuroki, N. J. *Polym. Sci. Polym. Chem. Ed.* **1973,** *11*, 1889.
3. Saraydin, D.; Karadag, E. *Rev. Roum. Chim.* **1998,** *43*, 139.
4. Voith, M. *Chem. Eng. News* **2010,** *88*, 22.
5. Cabasso, I.; Klein, E.; Smith, J. K. *J. Appl. Polym. Sci.* **1976,** *20*, 2377.
6. Ulbricht, M. *Polymer* **2006,** *47*, 2217.
7. Wang, D.; Li, K.; Teo, W. K. *J. Membr. Sci.* **1999,** *163*, 211.
8. Hood, D. K.; Tallon, M. A.; Clark, R. B.; Johnson, E. J. *J. Imag. Sci. Tech.* **2005,** *49*, 646.
9. Hood, D. K.; Kamin, S.; McKittrick, J. *Eur. Coatings J.* **2007,** *4*, 150.
10. He, D.; Susanto, H.; Ulbricht, M. *Progr. Polym. Sci.* **2009,** *34*, 62.
11. Yamagishi, H.; Crivello, J. V.; Belfort, G. *J. Membr. Sci.* **1995,** *105*, 237.
12. Reddy, B. S. R.; Soundararajan, S. *J. Appl. Polym. Sci.* **1991,** *43*, 251.
13. Sukhishvili, S. A.; Qiu, X. *J. Polym. Sci. Part A: Polym. Chem.* **2006,** *44*, 183.
14. Mauthauer, K.; Schneider, T.; Widmaier, R.; Kamm, A.; Bell, C.M. US 2007/0056900 A1 assigned to BASF **2007**.
15. Nagaoka, S.; Akashi, R. *Biomaterials* **1990,** *11*, 419.
16. Muller, H. J. US 7,300,022 B2 assigned to Siemens Water Technologies Corp. **2007**.
17. Hood, D. K. WO 2010/111607 A1 assigned to ISP Investments Inc. **2010**.
18. Hood, D. K.; Musa, O. M. WO 2009/023843 A1 assigned to ISP Investments Inc. **2009**.
19. Vilgis, T.; Winter, H. *Colloid Polym. Sci.* **1988,** *266*, 494.
20. Cates, M. J. *Phys. (Paris)* **1985,** *46*, 1059.
21. Stauffer, D. Introduction to Percolation Theory; Taylor and Francis: London, **1985,** p 1.
22. de Gennes, P. Scaling Concepts in Polymer Physics; Cornell University Press: Ithaca, New York, **1979.**
23. Lange, J.; Altman, N.; Kelly, C. T.; Halley, P. J. *Polymer* **2000,** *41*, 5949.
24. Larson, R. The Structure and Rheology of Complex Fluids; Oxford University Press: New York, **1999,** p 232.
25. Pugnaloni, L. A. arXiv.org eprint cond-mat/0406713, **2004.**
26. Hao, J.; Chan, L.; Shen, Z.; Heng, P. *Pharm. Dev. Technol.* **2004,** *9*, 379.
27. Chow, K. T.; Chan, L. W.; Heng, P. W. S. *Pharm. Res.* **2008,** *25*, 207.
28. Nerella, N.; Ulmer, H.; Chakrabarti, S.; Du Browny, G. US6129931 assigned to ISP Investments. **2000**.
29. Kim, U. Y.; Huang, R. Y. M. *Eur. Polym. J.* **1978,** *15*, 325.
30. Park, W. H.; Lee, J. K.; Kwon, K. J. *Polym. J.* **1996,** *28*, 407.
31. Chiniwalla, P.; Bai, Y.; Elce, E.; Shick, R.; McDougall, W. C.; Allen, S. A. B.; Kohl, P. A. *J. Appl. Polym. Sci.* **2003,** *89*, 568.